PLASMA DYNAMICS

V. GASEOUS ELECTRONICS

Academic and Research Staff

Prof. E. V. George
Prof. G. Bekefi
Prof. S. C. Brown
Dr. C. K. Rhodes
J. J. McCarthy
W. J. Mulligan

Graduate Students

W. J. Amisial
J. L. Miller
C. W. Werner
D. Wildman

A. KINETIC MODEL OF ULTRAVIOLET INVERSIONS IN HIGH-PRESSURE RARE GAS PLASMAS

Joint Services Electronics Program (Contract DAAB07-71-C-0300)

E. V. George, C. K. Rhodes

[Dr. C. K. Rhodes is supported under the auspices of the U.S. Atomic Energy Commission. His permanent address is: Department of Physics, Lawrence Livermore Laboratory, Livermore, California.]

Our studies of vacuum ultraviolet emission from high-pressure rare gases continue. We have expanded our kinetic model[1] to include the temperature dependence of the dissociative recombination coefficient α, as well as the thermal dissociation of both the molecular ion and excited dimer. We estimate the rate for these as follows.

O'Malley[2] has derived for α the temperature dependence of the dissociative recombination coefficient in the form

$$\alpha(T_e, T_v) = C\, T_e^{-1/2}[1 - \exp(-E_v/kT_v)],$$

where E_v is the vibrational quantum of the ion, T_e and T_v represent the electron and vibrational temperatures, and C is a constant.

Consider a typical molecular formation reaction of the form

$$Xe + Xe + Xe^+ \underset{k_B}{\overset{k_f}{\rightleftharpoons}} Xe_2^+ + Xe.$$

The forward rate coefficient k_f is known; we require an approximate form for the backward rate coefficient k_B. Using the principle of detailed balance, we obtain

$$k_B = k_f \left(\frac{\pi Me}{h^2}\right)^{-3/2} \left[(T_g)^{-1/2} \exp(-E_o/T_g)\right] T_v T_R,$$

where T_g, T_v, T_R are gas, vibration, and rotational temperatures in eV, and E_o is the dissociation energy of the molecule.

In our previous report,[1] we made the following basic assumptions in the calculation of this kinetic model. We assumed only single ionization so that $n_e = Xe_2^+ + Xe^+$ and gas kinetic, ion, and vibrational temperatures (T_g, T_+, T_v) are equal because of the high gas density. It was further assumed that the time evolution of the excited plasma is sufficiently rapid that the directed motion of the particles may be neglected (spatial homogeneity is assumed). This last assumption may not be valid in a laser-produced plasma subject to violent shock waves. We also neglected Bremsstrahlung cooling of the electron gas, and heat diffusion. We included the three-body electron-ion recombination mechanism which becomes important when sufficiently high electron densities are considered. Here we take an effective $\alpha = 10^{-10}$ cm^3/s.

A set of equations describing the time evolution of the electron, atomic ion, molecular ion, and excited-state densities, as well as the electron temperature T_e and the gas temperature T_g, was written. The resulting nonlinear differential equations were numerically integrated.

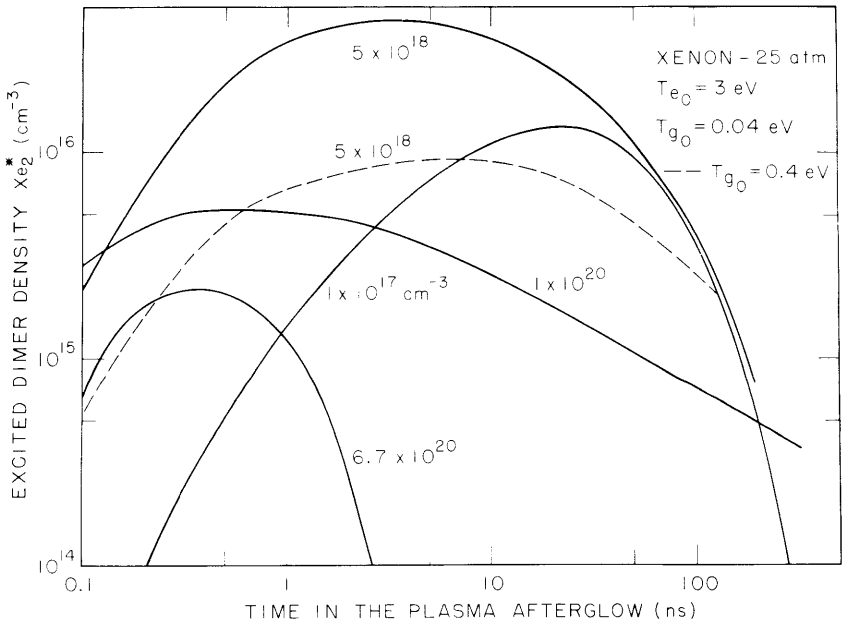

Fig. V-1. Time evolution of the excited dimer density corresponding to the $^3\Sigma_u^+$ state for various values of initial electron density n_{e_o}.

In Fig. V-1 we illustrate the time dependence of the excited dimer density ($^3\Sigma_u^+$ state) for various initial electron densities n_{e_o}. At time t = 0, defined to occur at the end of the primary plasma production pulse, the excited state and molecular ion densities were chosen to be ≈0 and the initial electron and gas temperatures were set equal to 3 eV and

0.04 eV, respectively. Notice that increasing n_{e_o} results initially in a larger excited dimer density (EDD) and that the peak EDD moves toward earlier times. One sees that there is an optimum value for n_{e_o} of $\sim 5 \times 10^{18}$ cm^{-3} (corresponding to a fractional ionization of approximately 1%). Further increase in n_{e_o} beyond the optimum results in a decreased peak EDD. This can be easily explained because energy is added to the gas in the process of dissociative recombination; that is, as n_{e_o} is increased a correspondingly greater amount of energy will be deposited in the gas. A higher T_g results in a decreased rate of production of the requisite excited atoms, as well as thermal dissociation of the excited dimers. The dashed line in Fig. V-1 shows the effect of a higher initial gas temperature on the temporal characteristics of the EDD for $n_{e_o} = 5 \times 10^{18}$.

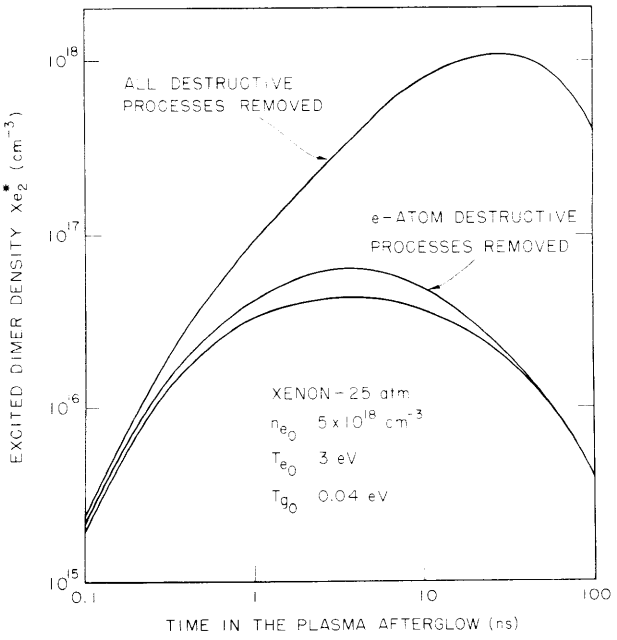

Fig. V-2. Effect of destructive processes on the time evolution of the excited dimer density.

We observe the expected result that a higher T_g results in a lower peak EDD. For the optimum n_{e_o} we find that 0.4% of the initial energy is stored in the $^3\Sigma_u^+$ state. To estimate the importance of the destructive processes,[3] the computer code was run with these processes suppressed. For the case $n_{e_o} = 5 \times 10^{18}$ we find (see Fig. V-2) that the peak EDD shifts to later times and increases by almost two orders of magnitude.

We note that since the stimulated emission cross section[4] of Xe_2^* is $\sim 3.5 \times 10^{-18}$ cm^2, an excited-state density of $\sim 10^{17}$ produces an optical gain coefficient of approximately

$0.4\ cm^{-1}$. For this excited-state density the loss from photoionization is small; however, the optical loss attributable to ground-state absorption[5] could be quite large. This loss, which is strongly temperature-dependent, is now being incorporated in our model.

In Fig. V-3 these calculations are compared with the measured intensity of the 1700 Å continuum emission from xenon. Experimentally,[6] the plasma is created by means of the passage of a pulsed relativistic electron beam (of 50 ns duration) through gaseous xenon at 1.1 atm pressure. The experimental result (solid line) shows two

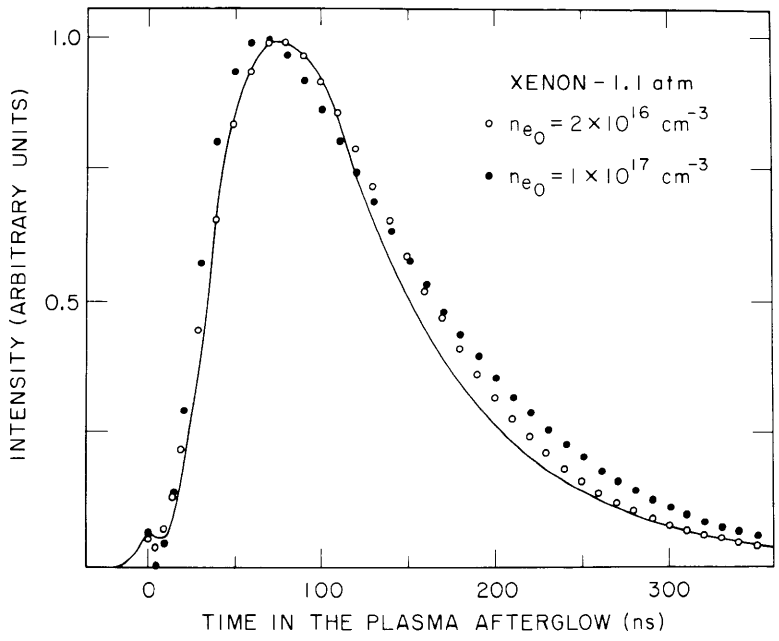

Fig. V-3. Comparison of the temporal characteristics of the observed 1700 Å continuum emission and our theoretical predictions. Data normalized to the second peak.

distinct peaks. The first peak is caused primarily by direct pumping processes, while the second, we feel, is the result of the recombinational process previously described. Here we estimated the initial excited-state densities (at t = 0) by using the ratio of the heights of the two experimental peaks. A lower bound for $n_{e_o} = 5 \times 10^{15}$ may be obtained by balancing the charged-particle production, using tabulated values[7] for the dE/dx of our beam, with recombinational losses. Notice that for $n_{e_o} = 2 \times 10^{16}$ the agreement between theory and experiment is good. Similar agreement has also been obtained for Ar and Kr using the correspondingly appropriate rate constants.

We have also included direct electron excitation and ionization using the cross

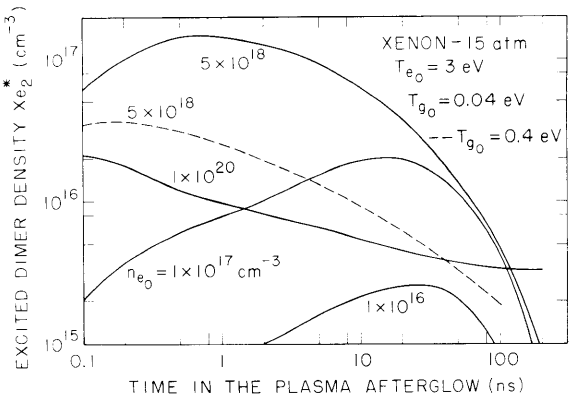

Fig. V-4. Time evolution of the excited dimer density for a model that includes direct electron excitation and ionization.

sections of Peterson and Allen.[8] Figure V-4 shows the time evolution of the excited dimer density for a model that includes these processes.

References

1. E. V. George and C. K. Rhodes, Quarterly Progress Report No. 108, Research Laboratory of Electronics, M. I. T., January 15, 1973, pp. 128-143.
2. T. F. O'Malley, Phys. Rev. 185, 101 (1969).
3. E. V. George and C. K. Rhodes, op. cit., see Equations (1) and (2).
4. A. V. Phelps, "Tunable Gas Lasers Utilizing Ground State Dissociation," JILA Report 110, University of Colorado, September 15, 1972.
5. R. E. M. Hedges, D. L. Drummond, and A. Gallagher, Phys. Rev. A 6, 1519 (1972).
6. B. Krawetz and C. K. Rhodes, "Vacuum Ultraviolet Studies of Rare Gases and Rare Gas Mixtures Excited with Pulsed High Energy Electron Beams," UCRL-73777, to be published in Proc. Symposium on High Power Molecular Lasers, Quebec City, May 15-17, 1972.
7. M. J. Berger and S. M. Steltzer, Tables of Energy Losses and Ranges of Electrons and Positrons, N65-12506 (NASA, Washington, D.C., 1964).
8. L. R. Peterson and J. E. Allen, Jr., J. Chem. Phys. 56, 6068 (1972).

B. MOLECULAR PROCESSES IN THE BREAKDOWN OF XENON GAS

Joint Services Electronics Program (Contract DAAB07-71-C-0300)

C. W. Werner

The conditions under which gaseous breakdown occurs have a profound effect upon subsequent electronic and molecular processes. In the study of xenon dimer formation, factors such as gas temperature, electron density, electron temperature, and rates of

excited state formation play a critical role. Most of our present theoretical and experimental research has been centered on direct-current excitation and breakdown of xenon gas.

Our previous studies (Quarterly Progress Report No. 108, pp. 128-149) were concerned for the most part with the afterglow of a xenon plasma. It was shown that under certain conditions, the density of an excited xenon dimer reached a substantial peak and that this peak was affected by the initial electron density and gas temperature. We are now investigating the feasibility of direct-current excitation as a route to these initial conditions in the afterglow.

During the breakdown, unlike the situation in the afterglow, excitations and ionizations from the ground state dominate the loss. They may be accounted for in our model by an addition to the rate equations:

$$\frac{dn_e}{dt} = n_e \nu_i + \text{(afterglow terms)}$$

$$\frac{dX^*}{dt} = n_e \nu_{ex} + \text{(afterglow terms)}.$$

Similarly, for the energy balance equation, we must add

$$\frac{d}{dt} n_e T_e = \text{(gain terms)} - \frac{2}{3} n_e \nu_i u_i - \frac{2}{3} n_e \sum \nu_{ex} u_{ex} + \text{(afterglow terms)}.$$

The gain term may be considered in several ways. A simple model assumes that the electrons come to equilibrium rapidly, and hence $T = T_o$ = constant for the duration of the excitation τ. Although this is a simple model and has the advantage of being independent of the mode of excitation (for example, dc, laser, microwave) the choice of arbitrary T_o and τ often leads to entirely unphysical results. This fact is apparent when the equations are integrated by computer. Very often, negative densities or temperatures are encountered when such assumptions are made.

Consequently, a more precise, although more restricted, model was necessary. If a simple dc field is assumed, the gain term becomes

$$\text{gain} = \frac{2}{3} n_e e v_d E$$

$$= \frac{2e^2E^2}{3m\nu_m}.$$

In general, the field E is a function of time. The first model assumed that E had the form of a square pulse. In this case, the electron temperature achieved its equilibrium value very rapidly as expected; however, the gas temperature in general rose

to extremely high values, sometimes exceeding that of the electron temperature. The reason for this is clear if we consider the implications of connecting a voltage source across the tube. By fixing E, the quantity of energy which can enter the system is unlimited. This becomes a problem at the point at which n_e is large, and substantial current is flowing. In such a case, the power dissipated into the tube exceeds any reasonable experimental value.

In the second modification of the model we took this limited available energy into

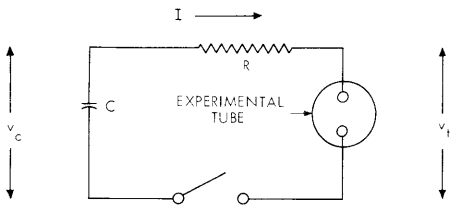

Fig. V-5.
Simple circuit model assumed for calculations.

account by assuming that a capacitor and a resistor were connected in series with the tube. At time t = 0, a switch was closed, and the voltage across the capacitor was applied to the tube (see Fig. V-5).

The current and voltages are related simply to the electron density

$$C \frac{dV}{dt} = -I$$

$$V_c - IR = V_t$$

$$= IR_t.$$

Hence we have the additional equation

$$\frac{dV_c}{dt} = - \frac{V_c}{C(R+R_t)}.$$

Now, $R_t = V_t/I$ and $I = JA$, where A is the cross-sectional area of the tube. If we assume that the field is constant, then the field $E = V_t/\ell$, where ℓ is the length. Employing the mobility, we arrive at the expression $R_t = \ell/e\mu An_e$, and thus $\frac{dV_c}{dt} = - \frac{V_c}{C(R+\ell/e\mu An_e)}$. The field across the tube is then simply defined by the relation $E = V_t/\ell = (V_c - IR)/\ell$. This field may be employed in the energy balance equation to calculate the quantities of interest. Since V_c is a function not only of time but also of n_e, it is necessary to integrate this equation by computer also. Results from this calculation

were checked by comparing experimentally observed currents with those predicted by theory. Experimentally, the current pulses appeared to be less intense and of greater duration than those predicted. Upon consideration of these facts, it seemed possible that this effect might be due to inductance in the circuit. Furthermore, ringing in the form of a negative undershoot on the trailing edge of the pulse was observed, which indicated that inductance was indeed present. The theoretical circuit was accordingly modified by including a voltage drop across an inductor equal to L dI/dt. Then the current, as well as the voltage, were integrated by the computer. Since the actual inductance of the experimental apparatus was a difficult parameter to measure, it was necessary to try several values in the program to see which one gave the best fit to the known results. Experimental vs theoretical values for the current are shown in Fig. V-6. Since the oscilloscope gives only a relative time measurement, the data were shifted to bring the peaks to the same time. It appears that the best theoretical fit of the data occurs for an inductance somewhere between 2 μH and 5 μH.

1. Optimization of Parameters

Ultimately we would like to achieve high densities of excited molecular dimers. By varying the parameters in the theory such as capacitance, resistance, and applied voltage, it is qualitatively possible to see what conditions are optimum.

An important factor is the initial voltage on the capacitor. To see what effect higher voltage has, we keep the initial energy in the capacitor a constant and raise the initial voltage in such a way that

$$CV^2/2 = \text{constant.}$$

Figure V-7 is the theoretical plot of Xe_2^* density against time for two cases. A characteristic feature of the density is that it shows several maxima and minima. In both cases there is a sharp peak followed by a very shallow peak which in turn is followed by a slow steady rise in density. In order to interpret the variety of peaks at least qualitatively, it is necessary to look at the densities of the other species. Figure V-8 is a graph of N/N_{max} for electrons and the two excited states that are considered in the model. The data are for V = 25 kV and C = 250 pF. It can be seen that excited states are directly pumped in the early stages before the electron densities become too large. These relatively high densities of excited states contribute to the first peak of Xe_2^*. Soon thereafter, the electron density rises to a peak, and dimer density drops sharply. This is probably due to electron collisions dissociating the molecule. At this point, excited states are also depleted because of ionization. As the capacitor discharges, the E/p of the tube drops, thereby causing the electrons to cool. The cooling now permits electrons to excite ground-state atoms selectively without ionizing them. Furthermore, dissociative

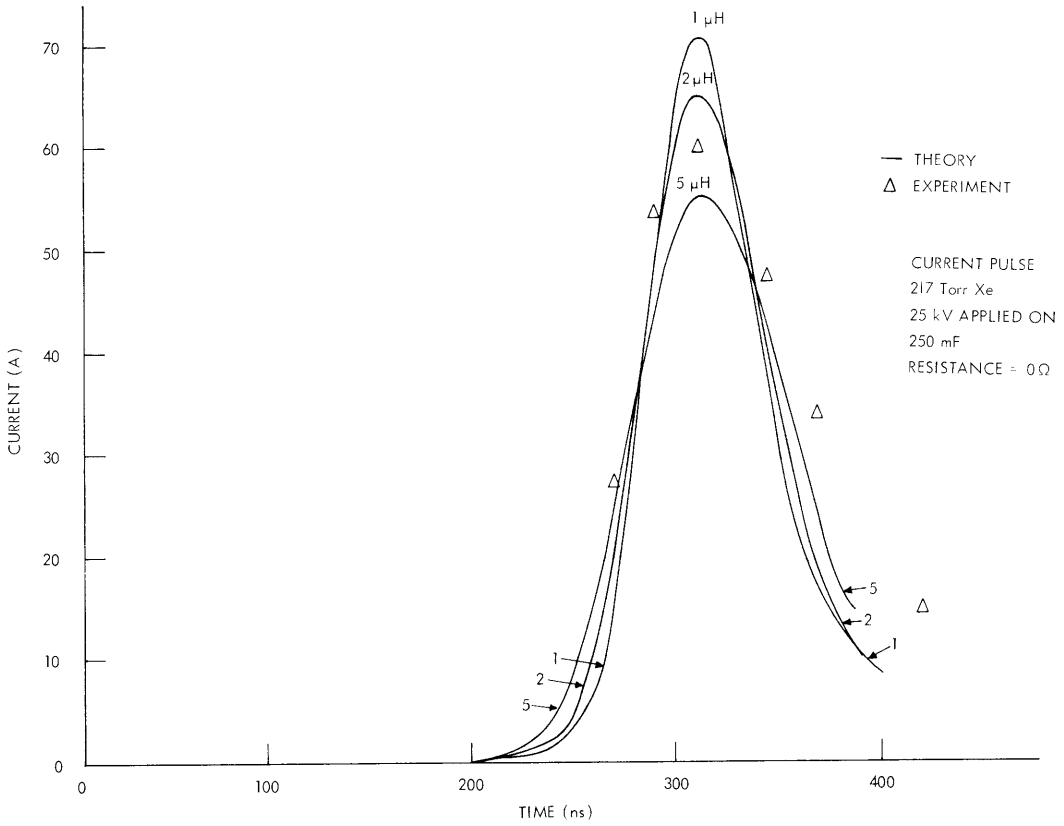

Fig. V-6. Current against time for various values of circuit inductance.

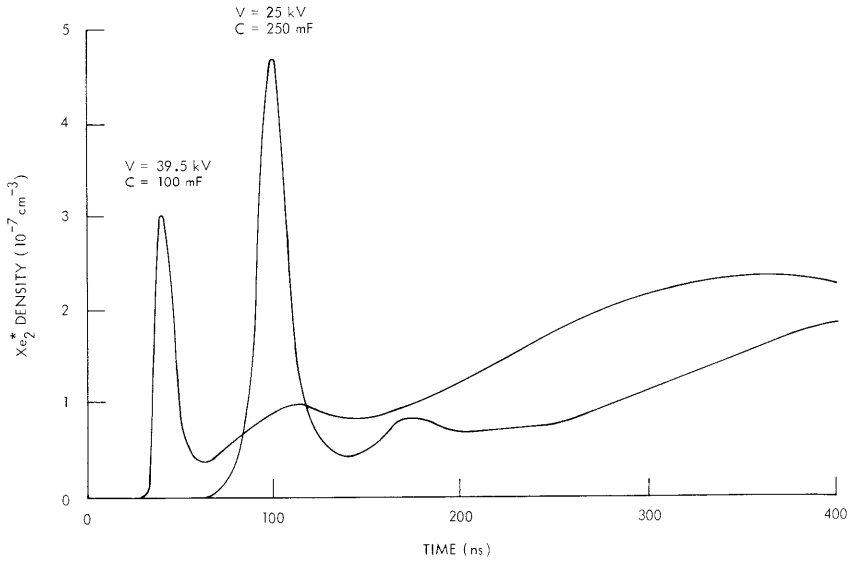

Fig. V-7. Dependence of Xe_2^* density on initial applied voltage.

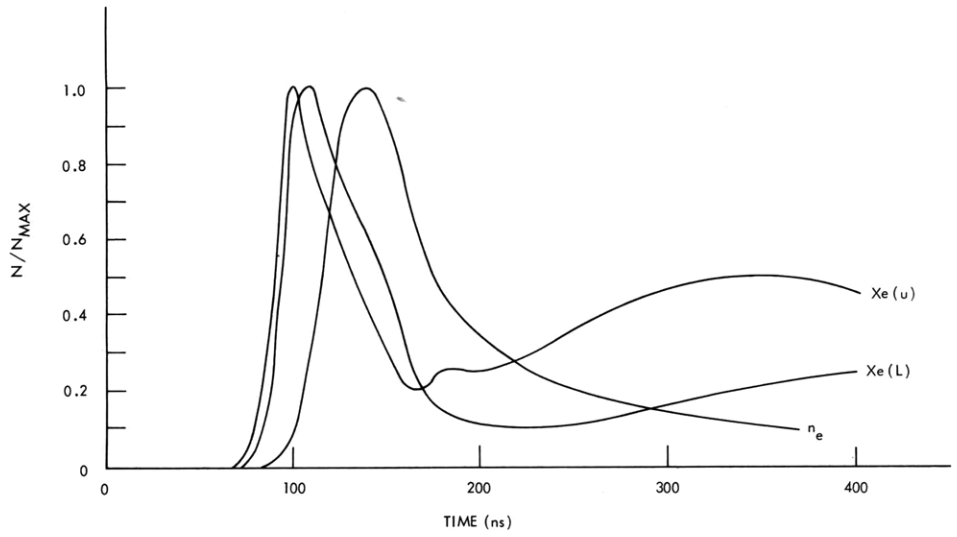

Fig. V-8. Relative densities of electrons and two excited states as a function of time.

recombination of the molecular ion now becomes an important feeding mechanism of the excited states. These factors undoubtedly account for the slow rise in the densities of dimer and excited states during the afterglow.

Experimentally, the measured light output shows a well-rounded peak which initially decays, but peaks again several hundred nanoseconds later (see Fig. V-9).

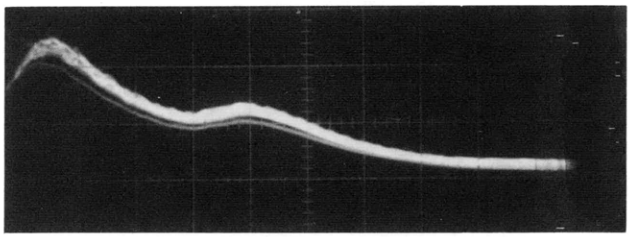

Fig. V-9. Experimental light output at 217 Torr.
Horizontal scale, 100 ns/cm.
Initial voltage, 25 kV.
Capacitance, 250 pF.
Length of tube, 18 cm.

Very simple spectral studies have been done on the light output, and are unmistakably continuum in nature for the first peak. Attempts to resolve spectral lines in the second peak have not been conclusive, largely because of the poor signal-to-noise ratio caused by pickup in the photomultiplier tube. Only after sufficient screening procedures

are employed will the spectra be particularly meaningful.

The first peak, being a continuum, is probably largely Bremsstrahlung and is obscuring the fine structure of early peaks in the dimer and metastable densities. It is probable, however, that the second peak can be attributed to the rise of both excited-state and molecular dimer densities in the afterglow.

It appears that increasing the initial voltage on the capacitor causes an increase in equilibrium electron temperature during the earlier stages of the pulse. The greater degree of ionization which results causes an increase in feeding of the lower states through dissociative recombination with the molecular ion in the afterglow. Merely increasing the energy input to the system by means of a larger capacitance actually has the opposite effect probably because of the gas heating which ensues. It seems that the optimum conditions for dimer formation are a low-energy, high-voltage pulse applied to the system for a short time. Investigations at higher pressures, including more detailed spectral analysis of light output, will be taken up in the future.